ULTRASONIC QUANTIFICATION OF THE TISSUE MICROSTRUCTURE OF SPONTANEOUS MAMMARY TUMORS IN RATS

Michael L. Oelze[1], James F. Zachary[2] and William D. O'Brien Jr.[1]

[1]Department of Electrical and Computer Engineering, [2]Department of Veterinary Pathology
University of Illinois at Urbana-Champaign

ABSTRACT

The quantification of tissue microstructure using ultrasound can aid in the detection and classification of disease. Eight retired breeder were acquired that had developed spontaneous mammary tumors. Two-dimensional B-mode images of the rat tumors were constructed from backscattered echoes. After scanning, tumors were dissected free from each rat, trimmed in the plane of ultrasound exposure, fixed in 10% neutral-buffered formalin, embedded in paraffin, sectioned at 5 μm, and stained with hematoxylin and eosin. Tumors were diagnosed microscopically as mammary gland fibroadenomas. Regions-of-interest (ROIs) were selected in the tumors and surrounding tissues and scatterer properties (average scatterer size and acoustic concentration) were estimated from the backscattered RF signal. Scatterer estimates were made by using least squares to fit a line to the measured form factor that was calculated from the backscattered power spectrum. Noise reduces the ability to make estimates of scatterer properties. A weighting scheme was used to reduce the effects of noise and increase the ability to make accurate estimates. Comparison of scatterer estimates made between normal tissues and tissues inside the tumors were made. On average, the estimated scatterer diameters inside the tumors were 30% larger at 107 micrometers than estimates of scatterer diameters outside the tumors averaging 82 micrometers. Similarly, the average acoustic concentration estimated inside the tumor was 3.16×10^{-2} mm^{-3} as opposed to 0.746 mm^{-3} for outside the tumor. In all but one of the rats, there was a statistically significant difference ($P < 0.05$) between estimates of scatterer properties made inside the tumors and in surrounding healthy tissues. Enhanced B-mode images were constructed by superimposing colored pixels that corresponding to the estimated scatterer properties on the gray-scale B-mode images. The enhanced B-mode images also showed differences between tissues inside and outside the tumors. (Supported by NIH CA 079179)

I. INTRODUCTION

Conventional B-mode images of tissues using ultrasound are made by relating the envelope-detected RF signal backscattered from the tissues to a grayscale. The frequency-dependent information contained in the backscattered RF signal is not utilized by conventional B-mode imaging. The frequency dependence has been hypothesized to contain information about tissue microstructure. Further examination of backscattered RF signals may yield parameterization about the tissue microstructure not resolved by conventional means.

Models have been used to relate frequency-dependent backscatter from tissues to microstructure [1,2]. The models have allowed estimates of average scatterer properties (size, shape and scatter strength) of tissue microstructure from backscattered RF signals for purposes of detecting and classifying tissues [2,3]. Parametric images created from estimates have been used to classify tissues [3,4,5]. Classification of tissues through parametric imaging techniques (noninvasive) is medically significant to diagnosis and treatment of disease.

In this work, a parametric imaging technique is explored and estimation schemes are optimized. The results are examined to determine the utility of the imaging technique for tissue classification.

II. THEORY

Gaussian scatterers have been used to model scattering from many soft tissues [6,7,8]. The theoretical power spectrum from a collection of Gaussian scatterers is, from Lizzi et al. [1],

$$W_{theor}(f) = \frac{185Lq^2 f^4 a_{eff}^6 n z_{rel}^2 e^{-12.59 f^2 a_{eff}^2}}{36\pi^4 \left[1 + 2.66\left(qfa_{eff}\right)^2\right]} \qquad (1)$$

where L is the gate length, f is frequency, q is ratio of transducer radius to distance from the ROI, nz_{rel}^2 is acoustic concentration and a_{eff} is the average effective radius of scatterers. Equation (1) takes into account the effects of the gating function (Hanning window) and transducer beam profile. The model assumes measurements are made in the depth of focus of a weakly focused transducer.

As sound propagates through tissues, sound is attenuated and scattered from small structures. Attenuation and scattering are frequency dependent. Furthermore, the initial excitation pulse assuming a Gaussian bandwidth, will be frequency dependent. Frequency components in the measured spectrum that have smaller magnitude due to the excitation bandwidth, attenuation and scattering will have smaller signal to noise ratio (SNR). Frequency components with small SNR can lead to inaccuracy in estimates of scatterer properties. Weighting different frequency components used in the scatterer property estimator according to their expected SNR can reduce the effects of the noise on estimates of scatterer properties. The SNR weighting has been applied to parametric images of the rat tumors, and reported herein.

III. EXPERIMENT

Spontaneous mammary tumors that had developed in eight Sprague-Dawley rats (Harlan, Indianapolis) were evaluated. The experimental protocol was approved by campus Laboratory Animal Care Advisory Committee and satisfied all campus and National Institutes of Health rules for humane use of laboratory animals. Each rat was euthanized and chest area was shaved with electric clippers and depilated. The rat was then placed on a holder in degassed water at 37° C for scanning.

A single-element weakly focused piston transducer was used to scan laterally across the tumors and surrounding tissues. The transducer had an aperture diameter of 12 mm and depth of focus of 50 mm. The center frequency of the transducer was 8 MHz with –6-dB pulse-echo bandwidth of 7 MHz. Estimates of scatterer properties were made within the depth of focus of the transducer. The transducer was operated in pulse-echo mode through a Panametrics 5800 pulser/receiver (Waltham, MA). The signals were recorded and digitized on an oscilloscope (Lecroy 9354 TM; Chestnut Ridge, NY) and downloaded to a PC computer for post-processing. The sampling rate was 50 MHz. The transducer was moved laterally across the chest and tumor by a micropositioning system with step size of a 100 μm between each A-line scan. The assumed attenuation was 0.9 dB/cm/MHz based on reports of attenuation measurements in the chest walls of rats [9].

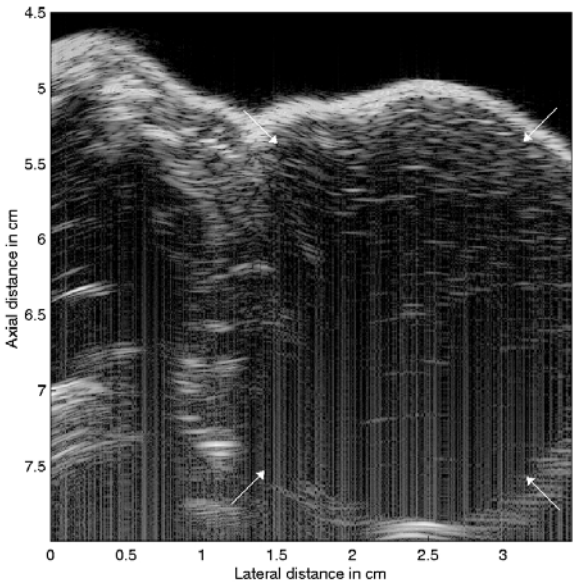

Figure 1 Grey-scale B-mode image of rat tumor and surrounding tissues. White arrows indicate tumor boundaries.

Grey-scale B-mode images were constructed from the ultrasonic scans. ROIs were selected from the B-mode images and used to estimate the scattering parameters. The ROIs were boxes 4 mm on a side. After making estimates from the power spectra from each ROI, parametric images were

constructed for each rat. The parametric images took the two properties estimated from each ROI and related the estimates to a particular colored pixel. The pixels were then superimposed on the conventional B-mode images to form two parametric images per rat. Figure 1 shows a conventional gray-scale B-mode image of a rat tumor and chest wall. Figures 2 and 3 show the parametric images of the same rat using the estimated scatterer properties.

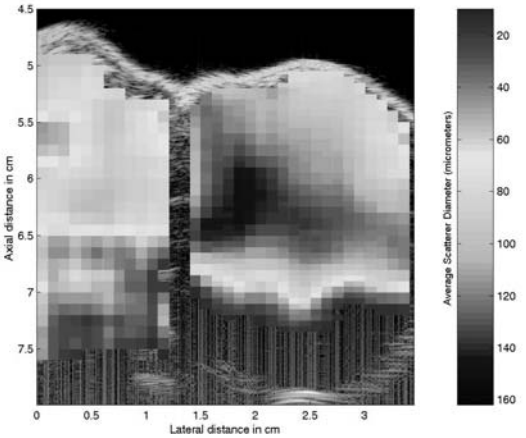

Figure 2 Parametric B-mode image with estimated average scatterer diameter (no SNR weighting).

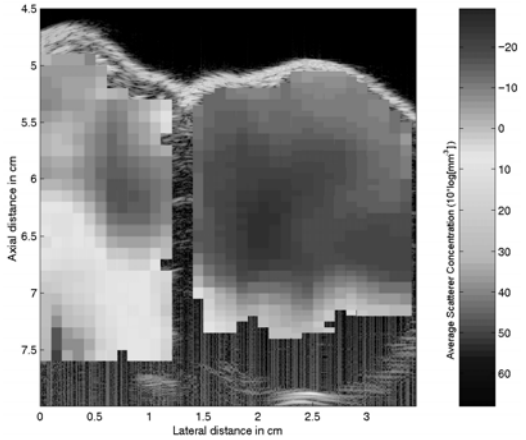

Figure 3 Parametric B-mode image with estimated average scatterer concentration (no SNR weighting).

The measured power spectrum from an individual ROI consisted of the averaged power spectra from several A-lines. Frequency-dependent attenuation was compensated in the measured power spectrum. Including the attenuation-compensation function, $A(f)$, and averaging over the ROI yielded for the measured power spectrum

$$W_{meas}(f) = \frac{R^2}{4} A(f) \frac{\langle W_m(f) \rangle}{W_{ref}(f)} \qquad (6)$$

where R is the reflection coefficient of the planar reflector in water. The planar reflector was used to obtain a calibration spectrum, $W_{ref}(f)$, to take out the effects of the equipment and settings on the measurement. The estimator used to obtain the scatterer properties was the best-fit line estimator by Oelze et al. [8].

The effects of the SNR weighting can be seen from the parametric image of Figure 4. The axial length of the tumor extends almost 2-½ cm in depth. The parametric image created without the SNR weighting (Figure 2) began to give increasingly smaller estimates at around 6.5 cm in depth until at around 7 to 7.1 cm estimates were unable to be made at all. The parametric image created with SNR weighting (Figure 4) allowed estimates of scatterer properties to be made throughout the full length of the tumor. The diagnostic capability was improved by using SNR weighting in the estimator.

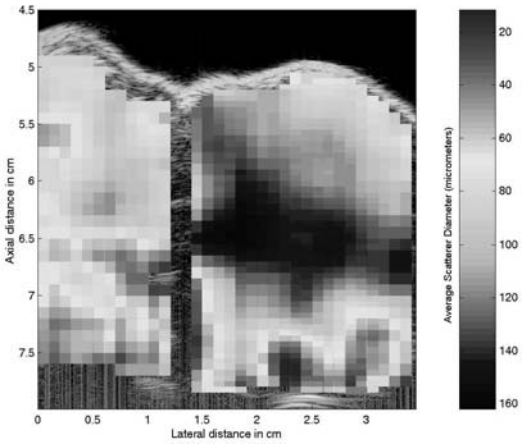

Figure 4 Parametric B-mode image with estimated average scatterer diameter (with SNR weighting).

To compare scatterer estimates in and outside the tumors with minimal effects from frequency-dependent attenuation losses, only the first half-centimeter in tissue depth was compared. The average scatterer diameters showed distinction between tissues in the tumor and in surrounding connective tissues. On average, there was a 30% difference between diameters estimated in the tumor and surrounding tissues. Estimates showed

there was a statistically significant difference between scatterer diameters in and out of the tumors (P = 0.0016) using ANOVA. Similar examination of average acoustic concentrations showed statistically significant difference between the tumor and surrounding tissues (P = 0.0014). A feature analysis plot of the estimated scatterer diameters versus acoustic concentrations is shown in Figure 5. The plot clearly shows a distinction between estimates of normal healthy tissues and tumor tissues.

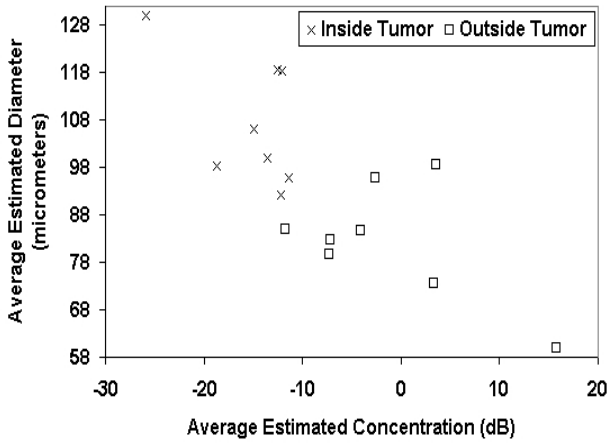

Figure 5 Feature analysis plot of estimated scatterer properties inside and outside the tumors.

IV. CONCLUSION

An estimation technique was used to estimate average scatterer diameters and concentrations in rats. Parametric images were constructed incorporating the scatterer property estimates. A weighting scheme was used in the estimator based on the expected SNR of different frequency components. The SNR weighting allowed the depth to which estimates could be made to increase. Examination of the scatterer property estimates inside and outside the tumors showed that the average scatterer diameter and acoustic concentration could be valuable as diagnostic indicators of disease.

V. REFERENCES

[1] F. L. Lizzi, M. Astor, T. Liu, C. Deng, D. J. Coleman, and R. H. Silverman, "Ultrasonic spectrum analysis for tissue assays and therapy evaluations," Int. J. Imaging Syst. Technol., **8**, 3-10 (1997).

[2] M. F. Insana, R. F. Wagner, D. G. Brown, and T. J. Hall, "Describing small-scale structure in random media using pulse-echo ultrasound," J. Acoust. Soc. Am., **87**, 179-192 (1990).

[3] M. F. Insana and T. J. Hall, "Parametric ultrasound imaging from backscatter coefficient measurements: image formation and interpretation," Ultrason Imaging, **12**, 245-267 (1990).

[4] J. A. Zagzebski, Z. F. Lu and L. X. Yao, "Quantitative ultrasound imaging: in vitro results in normal liver," Ultrason Imaging, **15**, 335-351 (1983).

[5] E. J. Feleppa, T. Liu, A. Kalisz, M. C. Shao, N. Fleshner and V. Reuter, "Ultrasonic spectral-parameter imaging of the prostate," Int. J. Imaging Syst. Technol., **8**, 11-25 (1997).

[6] D. Nicholas, "Evaluation of backscattering coefficients for excised human tissues: results, interpretation and associated measurements," Ultrasound Med. Biol., **8**, 17-28 (1982).

[7] D. K. Nassiri, and C. R. Hill, "The use of angular scattering measurements to estimate structural parameters of human and animal tissues," J. Acoust. Soc. Am., **87**, 179-192 (1990).

[8] M. L. Oelze, J. F. Zachary, and W. D. O'Brien Jr., "Characterization of tissue microstructure using ultrasonic backscatter: Theory and technique for optimization using a Gaussian form factor," J. Acoust. Soc. Am., **112**, 1202-1211 (2002).

[9] G. A. Teotica, R. J. Miller, L. A. Frizzell, J. F. Zachary, and W. D. O'Brien, Jr., "Attenuation coefficient estimates of mouse and rat chest wall," IEEE Trans. Ultrason., Ferroelect., Freq. Cont., **48**, 593-600 (2001).